

Article

Formation of CuO on TiO₂ Surface Using its Photocatalytic Activity

Hiromasa Nishikiori ^{1,2,*}, Naoya Harata ¹, Saho Yamaguchi ¹, Takashi Ishikawa ¹, Hayato Kondo ¹, Ayaka Kikuchi ¹, Tomohiko Yamakami ¹ and Katsuya Teshima ^{1,2}

¹ Faculty of Engineering, Shinshu University, 4-17-1 Wakasato, Nagano 380-8553, Japan; naoya.harata@yahoo.com (N.H.); saho.yamaguchi@yahoo.com (S.Y.); takashiishikawa222@yahoo.com (T.I.); hayato.k0716@gmail.com (H.K.); aykikuchi@shinshu-u.ac.jp (A.K.); tyamaka@shinshu-u.ac.jp (T.Y.); teshima@shinshu-u.ac.jp (K.T.)

² Center for Energy and Environmental Science, Shinshu University, 4-17-1 Wakasato, Nagano 380-8553, Japan

* Correspondence: nishiki@shinshu-u.ac.jp; Tel.: +81-26-269-5536

Received: 3 April 2019; Accepted: 22 April 2019; Published: 24 April 2019



Abstract: Some co-catalyst nanoparticles can enhance the activity of photocatalysts due to prolonging the charge separation lifetime by promoting the electron or hole transfer. CuO particles were prepared from an aqueous solution of copper (II) nitrate at 351 K on a TiO₂ surface by a photocatalytic reaction and heating at 573 or 673 K. The amount and size of the particles deposited during the photocatalytic reaction can be controlled by changing the amount of the irradiated photons. The CuO crystals with about 50–250 nm-sized particles were formed. Nitrate ions were reduced to nitrite ions in the solution by the photocatalytic activity of the TiO₂, and water was simultaneously transformed into hydroxide ions. An increase in the basicity on the TiO₂ surface induced formation of a copper hydroxide. The copper hydroxide was subsequently dehydrated and transformed into CuO by heating. The TiO₂ loading of a small amount of CuO demonstrated a higher photocatalytic activity for methylene blue degradation compared to the original TiO₂ due to the electron transfer from the TiO₂ conduction bands to the CuO conduction band.

Keywords: CuO; TiO₂; photocatalytic deposition; surface modification; photocatalysis

1. Introduction

Titanium dioxide (TiO₂) is modified with some co-catalysts in order to improve its photocatalytic activity due to prolonging the charge separation lifetime by promoting the electron or hole transfer [1,2]. For this purpose, noble metals and their oxides are frequently used as the modifiers to trap the electrons in the conduction band and holes in the valence band, which suppresses the electron–hole charge recombination [1–3]. Recently, the non-noble metals or their oxides, such as Ni, Co, NiO_x, and CoO_x, are also used as co-catalysts. The conduction and valence bands of such semi-conductive metal oxides can trap the charges. Furthermore, CuO_x and Cu(OH)₂ can also be a substitute for them [4–13]. The electron transfer from the TiO₂ conduction bands to the CuO conduction band enhances the photocatalytic activity because it suppresses the charge recombination on the TiO₂ and promotes oxidation on the TiO₂ by the hole and reduction on the CuO by the transferred electron. CuO is also useful as a visible-light-driven photocatalyst [4,6,8,10–13].

One of the photocatalysts, zinc oxide (ZnO) particles, was previously deposited from an aqueous zinc nitrate solution at 323–358 K on a TiO₂ thin film by its photocatalytic activity [14,15]. On the other hand, the growth of the anatase TiO₂ nanoparticles on its film was observed in a solution containing titanium (IV) chloride and lithium nitrate maintained at 353 K during UV irradiation [16]. Anatase TiO₂ crystals with the size of ca. 20 nm were produced on the original TiO₂ film composed of the

particles with almost the same size. Silica nanolayers were also formed as adsorbents on the anatase TiO₂ particles immersed in solutions of tetraethyl orthosilicate (TEOS) during the UV irradiation [17].

The nitrate ions were reduced to nitrite ions in the solution, and water was simultaneously transformed into hydroxide ions ($\text{NO}_3^- + \text{H}_2\text{O} + 2\text{e}^- \rightarrow \text{NO}_2^- + 2\text{OH}^-$) by a photocatalytic reduction reaction on the original TiO₂ film, as previously reported [14–16]. According to this mechanism, an increase in the basicity on the TiO₂ surface induced the hydroxide formation. The hydroxides were subsequently dehydrated and transformed into the oxides. On the other hand, the UV irradiation caused a slight increase in the density of the basic OH groups on the TiO₂ surface [18–20]. Even if there is a slight increase in the basicity it promotes hydrolysis of the TEOS and subsequent polymerization of its products, then the silica layers are deposited on the TiO₂ surface [17]. The amount and size of the particles deposited during the photocatalytic reaction can be controlled by changing the amount of the irradiated photons as studied in the ZnO, TiO₂, and silica formation [14–17]. Therefore, this is suitable for forming co-catalyst nanoparticles selectively on the photoactive sites of the original photocatalyst particles, as distinct from the other methods.

In this study, CuO nanoparticles were also attempted to be formed from an aqueous solution of Cu (II) nitrate on a substrate plate coated with a TiO₂ thin layer by a photocatalytic reaction based on such a preparation process of the mentioned oxides. The difficulty of the metal oxide formation depends on that of the dehydration of the metal hydroxides. It is an important point as to whether the dehydration of the copper hydroxide can proceed in the aqueous solution, although the silicon, zinc, and titanium hydroxides were easily dehydrated. The photocatalytic activity of the CuO-modified TiO₂ and the co-catalyst function of the CuO were evaluated by a normal dye degradation during UV irradiation.

2. Results and Discussion

2.1. Characterization of the Film Surface

The objective samples were prepared on the glass substrate plates with the TiO₂ thin layer for observations of their microscopic morphology and crystal structure of the particles deposited during the UV irradiation. As previously observed, the surface SEM image indicated that the pre-coated TiO₂ film was composed of particles with the size of ca. 20 nm [14,15]. The Raman spectrum of the film corresponded to that of the standard sample of anatase TiO₂. No peak was, however, detected on the substrate by the XRD analysis due to the thinness of the TiO₂ layer. Figure S1 shows the element mapping images of the Ag-deposited TiO₂ film obtained by electron probe microanalysis (EPMA). The Ag particles were dispersed on the film surface. The elemental ratio of Ag/Ti was 0.74 and a sufficient amount for the co-catalyst of TiO₂.

No XRD peak was observed on the samples prepared in the dark or on the glass substrates without the Ag-deposited TiO₂ film even during the UV irradiation. The characteristic peaks were observed in the XRD patterns of the unheated samples prepared from the solutions of pH 3.07, pH 3.90, and pH 4.57 on the Ag-deposited TiO₂ films during the UV irradiation, as shown in Figure 1. All the samples exhibited peaks at $2\theta = 12.8^\circ$ and 25.7° assigned to the (001) and (200) planes, respectively, of Cu₂(OH)₃(NO₃), i.e., layered copper hydroxide (LCH) nitrate [21,22]. CuO was not observed under the present conditions similar to the layered zinc hydroxide (LZH) nitrate in the case of the ZnO formation [14,15]. The LCH was reported to be formed in a basic solution and decomposed to CuO during heating at 333–508 K [23]. The LCH formation indicated that the dehydration did not proceed due to a very low reaction rate in the solution. The sample prepared from the solution of pH 3.07 also exhibited a halo peak assigned to amorphous copper hydroxides in addition to the above peaks due to the slow reaction. The average LCH crystallite sizes were estimated from the full width at half maximum (FWHM) of the (001) peak using Scherrer's equation. The sizes of the crystallites produced from the solutions of pH 3.07, pH 3.90, and pH 4.57 were 29.6, 32.0, and 32.0 nm, respectively. The sizes are determined by the rates of the crystal nucleus formation and crystal growth as reported in the previous study of the photocatalyzed ZnO formation [15]. A higher pH generally induces the

forming of a greater amount of LCH nuclei in the solution. However, the amounts of the crystal nuclei significantly depend on the amount of the Ag particles on the TiO₂ surface. The higher pH can better promote the crystal growth in this case. Under the present conditions, dehydration of the LCH was more difficult than that of zinc and titanium hydroxides because CuO is more easily hydrolyzed.

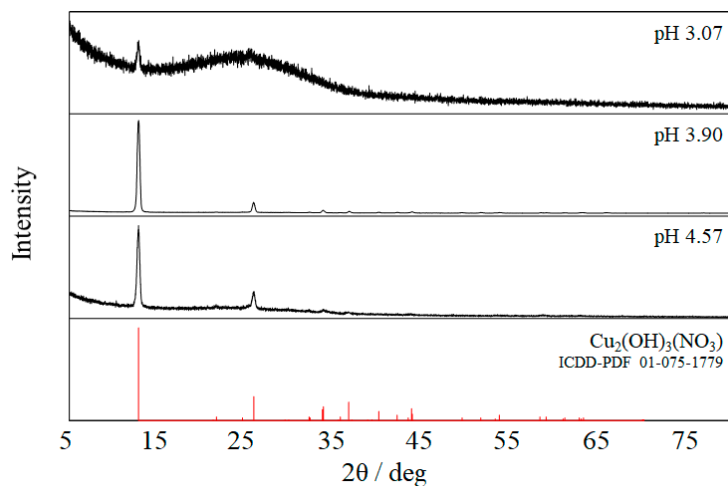


Figure 1. XRD patterns of the unheated samples prepared from the solutions of pH 3.07, pH 3.90, and pH 4.57.

The EPMA element mapping images of the unheated samples prepared from the solutions of pH 3.07, pH 3.90, and pH 4.57 were obtained as shown in Figure 2. In the sample prepared from the solution of pH 3.07, the amount of the Cu element was lower than the lower detection limit although its XRD pattern indicated the formation of LCH. This is because a slight amount of LCH was dispersed on the TiO₂ film. The Cu/Ti element ratios of these samples prepared from the solutions of pH 3.90 and pH 4.57 were 0.51 and 0.27, respectively. In the sample prepared from the solution of pH 3.90, the elemental Cu was distributed in a limited area. Only a slight amount of the elemental Cu was observed in almost all of the areas. In the sample prepared from the solution of pH 4.57, the elemental Cu was widely distributed over the entire area.

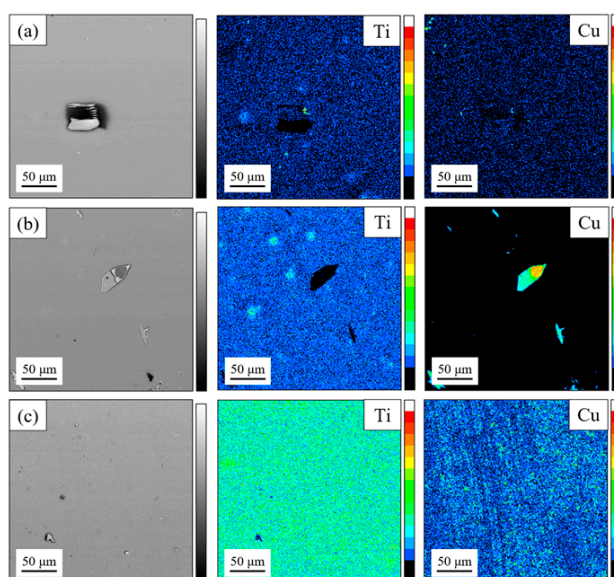


Figure 2. EPMA element mapping images of the unheated samples prepared from the solutions of (a) pH 3.07, (b) pH 3.90, and (c) pH 4.57.

Figure 3 shows the XRD patterns of the samples prepared from the solutions of pH 3.07, pH 3.90, and pH 4.57 and heated at 673 K for 2 h. No peak was clearly observed in the XRD pattern of the sample prepared from the solution of pH 3.07. A slight amount of LCH was partially dehydrated, but not completely transformed into CuO, thus being possibly amorphous copper hydroxides due to the strong hydration. In the sample prepared from the solution of pH 3.90, LCH was still observed. A small amount of LCH was presumed to be stably stacked in small cavities on the TiO₂ film surface. The samples prepared from the solutions of pH 3.90 and pH 4.57 exhibited peaks at $2\theta = 32.5^\circ, 35.5^\circ, 38.8^\circ, 48.7^\circ, 53.5^\circ, 58.5^\circ, 61.5^\circ, 65.9^\circ, 66.2^\circ, 68.1^\circ,$ and 68.2° assigned to the (110), (002), (111), ($\bar{2}02$), (112), (202), ($\bar{1}13$), (022), ($\bar{3}11$), (113), and (220) planes of CuO, respectively. The average CuO crystallite sizes were estimated from the FWHM of the (002) peak using Scherrer's equation. The sizes of the crystallites produced from the solutions of pH 3.90 and pH 4.57 were 21.0 and 19.3 nm, respectively. These results indicated that the UV irradiation induced the photocatalytic formation of copper hydroxide on the TiO₂ film and the additional heat mainly accelerated its dehydration and transformation into CuO [23].

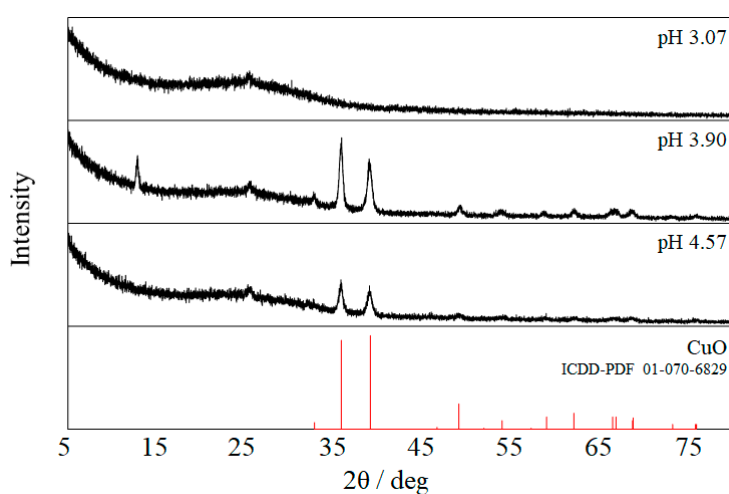


Figure 3. XRD patterns of the samples prepared from the solutions of pH 3.07, pH 3.90, and pH 4.57 and heated at 673 K for 2 h.

Figure 4 shows the SEM images of the samples prepared from the solutions of pH 3.07, pH 3.90, and pH 4.57 and heated at 673 K for 2 h. Under the condition of pH 3.07, island-like deposits with the size of ca. 2 μm were observed on the film. However, almost all of these are presumed not to be copper compounds because a slight amount of them was detected by the EPMA. Small amounts of TiO₂ aggregates were possibly reconstructed during the UV irradiation. Under the condition of pH 3.90, the CuO particles with the sizes of 100–300 nm were aggregated on the TiO₂ films. The aggregates of the amorphous or low crystalline particles were deposited at a low pH similar to the case of the ZnO formation [15]. Under the condition of pH 4.57, the second-order particles of the aggregates with ca. 50-nm sized CuO particles were dispersed on the TiO₂ film.

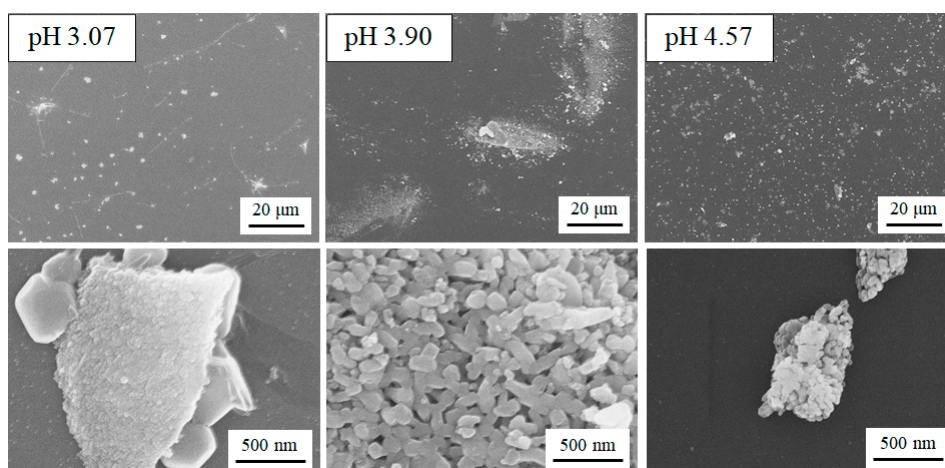


Figure 4. SEM images of the samples prepared from the solutions of pH 3.07, pH 3.90, and pH 4.57 and heated at 673 K for 2 h.

Figure 5 shows the XRD patterns of the samples prepared from the solutions of pH 4.57 and heated at 373, 473, 573, and 673 K for 2 h. The samples heated at 373 and 473 K still retained the LCH peaks while those heated at 573 and 673 K exhibited the CuO peaks. The average crystallite sizes of the samples heated at 573 and 673 K were 20.7 and 19.3 nm, respectively, which were almost the same. The temperature corresponding to the thermal energy for dehydration of the LCH particles was 473–573 K under the present conditions. This is consistent with the reported results [23]. The CuO formation required a specific pH condition for the reaction solution and heating temperature for the deposits.

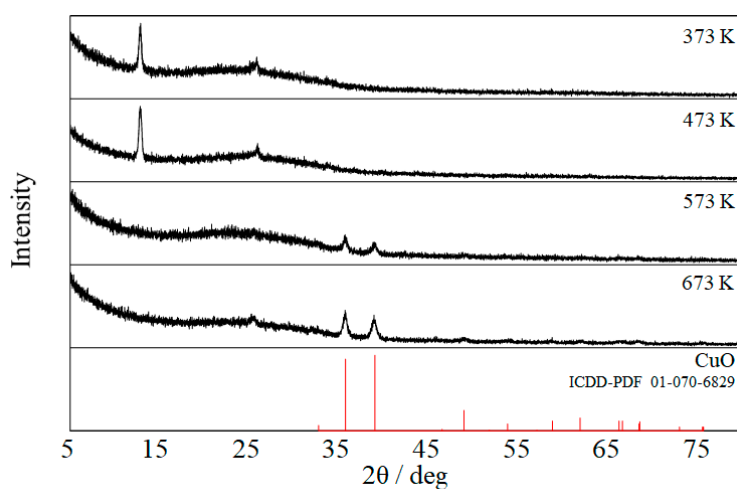


Figure 5. XRD patterns of the samples prepared from the solutions of pH 4.57 and heated at 373, 473, 573, and 673 K for 2 h.

Figure 6 shows the SEM images of the samples prepared from the solutions of pH 4.57 and heated at 373, 473, 573, and 673 K for 2 h. The particles were highly dispersed on the TiO₂ film surface in all the samples. The particles with the sizes of 100–250 nm and ca. 50 nm were observed in the samples containing the LCH and CuO, respectively. The aggregates of the particles were dispersed on the TiO₂ film surface. The more hydrophilic LCH particles more easily formed aggregates. The CuO nanocrystals were formed by the photocatalytic reaction and heating, although their shape was difficult to control.

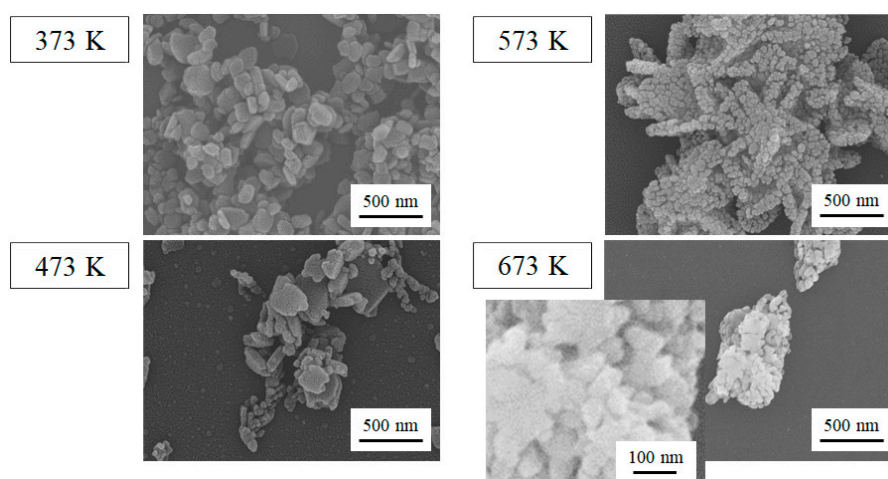


Figure 6. SEM images of the samples prepared from the solutions of pH 4.57 and heated at 373, 473, 573, and 673 K for 2 h.

2.2. Photocatalytic Activity of the CuO-Modified TiO₂ Powders

The photocatalytic activities of the CuO-modified TiO₂ films were lower than that of the original TiO₂ film because the amount of the CuO was too great to enhance the charge separation, which significantly prevented light absorption of the TiO₂. This study aims to form the CuO nanoparticles on the TiO₂ as the co-catalyst rather than the counterpart semiconductor for the heterojunction. Furthermore, the powder sample is more suitable to evaluate the photocatalytic activity for organic molecule degradation due to the effective surface area contacting them. A lower amount of the CuO was deposited on the TiO₂ powder without any Ag particles in order to confirm the enhancement of the photocatalytic activity by the modification.

Table 1 shows the Cu/Ti ratio of the powder samples prepared using the 0.500–100 mmol dm^{−3} Cu(NO₃)₂ solutions and heated at 573 K for 2 h, which was estimated by EPMA. The Cu amount of these samples was smaller than the resolution limit of the EPMA element mapping. Figure 7 shows the more highly resolute images of the SEM-EDS element mapping of the powder sample prepared using the 0.500 mmol dm^{−3} Cu(NO₃)₂ solution and heated at 573 K for 2 h. The elemental Cu was highly dispersed on the TiO₂ surface. However, the surface of the modified TiO₂ particles was not significantly distinct from the original TiO₂ surface based on even their TEM images similar to the TiO₂ modified with silica by the photocatalytic reaction [17]. If it is postulated that a TiO₂ cubic particle with the size of 20 nm is covered with a 0.1 nm-thick CuO monolayer, the Cu/Ti ratio of the TiO₂ particle loading the CuO monolayer can be estimated by a simple calculation to be about 3%. The samples prepared using less than 100 mmol dm^{−3} Cu(NO₃)₂ solutions can load submonolayers or very small nanoparticles of CuO. Figure S2 shows the XPS spectra related to the Cu 2p electrons for the original and modified TiO₂ samples [6,7,10–13]. The modified TiO₂ samples exhibited the Cu 2p_{2/3} peaks at around 934 eV assigned to Cu²⁺ of CuO. The BET specific surface area for the original TiO₂ and CuO-modified TiO₂ powders are shown in Table 2. The specific surface area for the TiO₂ powders modified using the 0.500 and 1.00 mmol dm^{−3} Cu(NO₃)₂ solutions was not significantly distinct from that for the original TiO₂ powder (49 m² g^{−1}) because the amount of the deposited CuO was very low. The specific surface area clearly decreased by the modification using the 10.0 and 100 mmol dm^{−3} Cu(NO₃)₂ solutions due to the CuO aggregation.

Table 1. Cu/Ti ratio of the powder samples prepared using the 0.500–100 mmol dm^{−3} Cu(NO₃)₂ solutions and heated at 573 K for 2 h. Each elemental composition was estimated by EPMA.

Cu(NO ₃) ₂ /mmol dm ^{−3}	0.500	1.00	10.0	100
Cu/Ti ratio	0.22%	0.67%	1.30%	7.98%



Figure 7. SEM-EDS element mapping images of the powder sample prepared using the $0.500 \text{ mmol dm}^{-3}$ $\text{Cu}(\text{NO}_3)_2$ solution and heated at 573 K for 2 h.

Table 2. BET specific surface area of the TiO_2 powder sample and the powder samples prepared using the $0.500\text{--}100 \text{ mmol dm}^{-3}$ $\text{Cu}(\text{NO}_3)_2$ solutions and heated at 573 K for 2 h.

$\text{Cu}(\text{NO}_3)_2/\text{mmol dm}^{-3}$	0	0.500	1.00	10.0	100
Specific surface area ($\text{m}^2 \text{g}^{-1}$)	49 ± 5	52 ± 4	57 ± 3	40 ± 1	28 ± 1

Figure S3 shows the UV–Vis diffuse reflectance spectra of the TiO_2 and CuO -modified TiO_2 samples. The ordinate indicates the Kubelka–Munk function approximating the absorbance. As expected, the absorption edge of the original TiO_2 sample is located at around 400 nm. The CuO -modified TiO_2 samples clearly exhibit a visible light absorption at around 400–500 nm, the intensity of which increased with an increase in the loading amount of the CuO .

Figure S4 shows the changes in the concentration of methylene blue (MB) during the UV irradiation using the TiO_2 and CuO -modified TiO_2 powder samples. Figure 8 shows the plots of the quasi first-order reaction analysis of them. The concentration is normalized by each adsorption equilibrium concentration on the powder samples. Figure 9 shows the adsorption amounts and degradation rate constants of MB on the TiO_2 powder and the powders prepared using the $0.500\text{--}100 \text{ mmol dm}^{-3}$ $\text{Cu}(\text{NO}_3)_2$ solutions. The adsorption and degradation properties on the latter powders were evaluated before (copper hydroxides) and after (CuO) heating them. The adsorption amounts somewhat decreased by heating due to a decrease in the hydrophilicity of the surface. On the other hand, the degradation rate increased by heating due to the CuO formation. CuO functioned as a co-catalyst better than the copper hydroxide in this study. The amount of the MB adsorbed on the unheated samples in the dark increased and decreased with an increase in a loading amount of the Cu . The degradation rate constants on the samples also increased and decreased corresponding to their adsorption properties. On the other hand, the amount of the MB adsorbed on the heated samples was lower in the samples loading a large amount of the CuO . The samples with the Cu contents of 0.67% and 1.30% exhibited higher activities than the original TiO_2 . These samples had a submonolayer of CuO and areas larger than 75% of the TiO_2 particle surface can be bare. The greater CuO should lower the photocatalytic activity of the TiO_2 because it prevented light absorption of the TiO_2 and transfer of the separated charges to the reactants adsorbed on the particle surface. In previous examples, the samples with the CuO contents of 1%–5% exhibited the highest activity of all the samples [6,10,13]. Therefore, the TiO_2 loading a small amount of CuO demonstrated a higher photocatalytic activity for degradation of the organic dye compared to the original TiO_2 .

Figure S5 shows the relative concentrations of MB and TOC after the photocatalytic degradation for 60 min using the TiO_2 sample and the CuO -modified TiO_2 samples prepared using the 1.00 and $10.0 \text{ mmol dm}^{-3}$ $\text{Cu}(\text{NO}_3)_2$ solutions. The relative concentrations were calculated by normalizing the initial concentrations estimated by the UV–Vis absorption and TOC measurements. The concentrations estimated by the TOC analysis were higher than those estimated by the UV–Vis spectroscopy by 10%–20%. This result indicated that some MB molecules were not completely mineralized, but partially degraded to colorless organic species, as reported [24,25].

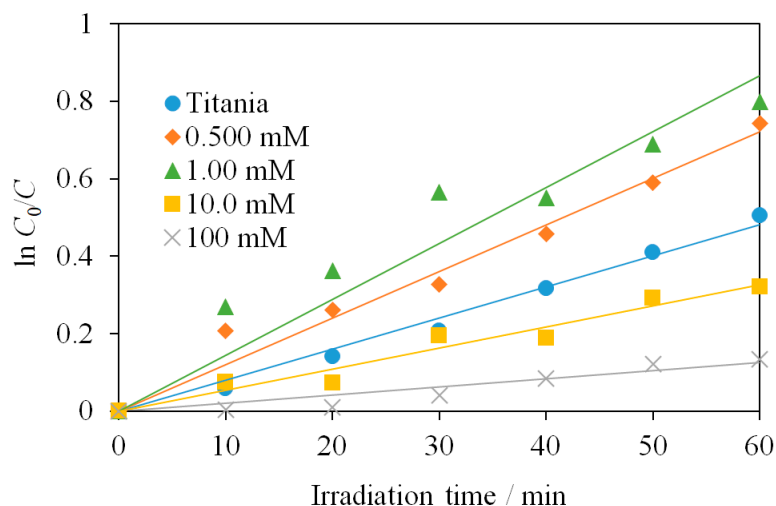


Figure 8. Quasi first-order reaction analysis of the changes in the MB concentration during the UV irradiation (300–400 nm, peak at 352 nm, $40 \mu\text{W cm}^{-2}$) using the TiO_2 sample and the CuO -modified TiO_2 samples prepared using the 0.500–100 mmol dm^{-3} $\text{Cu}(\text{NO}_3)_2$ solutions.

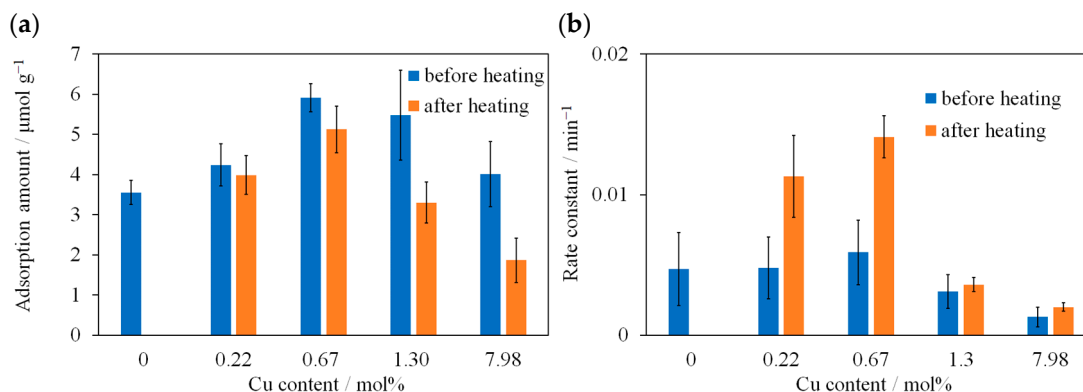
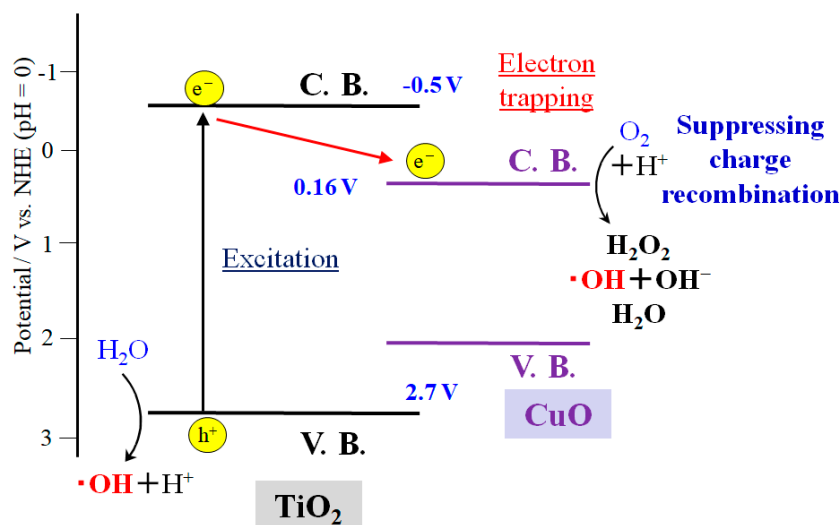


Figure 9. (a) Adsorption amounts and (b) degradation rate constants of MB using the TiO_2 powder and the powders prepared using the 0.500–100 mmol dm^{-3} $\text{Cu}(\text{NO}_3)_2$ solutions. The adsorption and degradation properties on the latter powders were evaluated before and after heating them.

Figure S6 shows the change in the fluorescence intensity of 2-hydroxy terephthalic acid resulting from hydroxyl radical trapping during the UV irradiation using the TiO_2 film and the CuO -modified TiO_2 film prepared using the 100 mmol dm^{-3} $\text{Cu}(\text{NO}_3)_2$ solution and the TiO_2 powder and the CuO -modified TiO_2 powder prepared using the 1.00 mmol dm^{-3} $\text{Cu}(\text{NO}_3)_2$ solution. These CuO -modified TiO_2 samples were prepared by heating at 573 K. An energy diagram of the photocatalytic reaction on the CuO -modified TiO_2 is shown in Scheme 1. Hydroxyl radical originating from the photocatalytic water oxidation and oxygen reduction is an active species degrading organic molecules. The present fluorescence analysis is a method to evaluate enhancement of the hydroxyl radical formation, which was promoted by the electrons transferred from the TiO_2 conduction bands to the CuO conduction band due to suppressing the charge recombination [26,27]. The production rate of hydroxyl radical of the CuO -modified TiO_2 film was slower than that of the original TiO_2 film, while that of the CuO -modified TiO_2 powder was clearly faster than that of the original TiO_2 powder. These results corresponded to those of the MB degradation. Therefore, the charge separation efficiency is significant for the production of the activate species.



Scheme 1. Energy diagram of photocatalytic reaction on CuO-modified TiO₂ in water.

3. Materials and Methods

3.1. Sample Preparation

Aqueous solutions of 0.100 mol dm⁻³ copper (II) nitrate trihydrate (Cu(NO₃)₂·3H₂O, Wako, Osaka, Japan, S grade) were prepared in which the pH was adjusted to 3.1–4.6 with nitric acid and sodium hydroxide (Wako, Osaka, Japan, S grade). The glass substrates (Matsunami, Kishiwada, Japan, S-1111) were dip-coated with a very thin TiO₂ layer by the sol–gel method. For preparation of the sol, 25.0 cm³ of ethanol (Wako, Osaka, Japan, S grade), 0.21 cm³ of nitric acid, and 0.21 cm³ of water were mixed, followed by adding 5.0 cm³ of titanium tetraisopropoxide (Wako, Osaka, Japan, reagent grade) in a dry nitrogen atmosphere. Water was ion-exchanged and distilled by a distiller (Yamato, Tokyo, Japan, WG23). The anatase TiO₂ films were formed by three dip-coatings using the sol, followed by heating at 773K for 30 min. The thickness of the TiO₂ film was ca. 50 nm, as previously reported [15].

The light irradiation for the sample preparation was conducted as previously reported [17]. The glass substrates with the TiO₂ film were immersed in water along with light irradiation for 20 min in order to remove any organic compounds on the surface. They were then immersed in an aqueous solution of 60.0 mmol dm⁻³ silver nitrate (AgCl, Wako, Osaka, Japan, S grade) during nitrogen gas purging for 5 min in order to remove the dissolved oxygen, then light irradiation for 40 min in order to deposit Ag particles. Consequently, Ag particles were slightly formed on the surface to function as nuclei for the CuO crystal growth and as the promoter for the TiO₂ photocatalyst. Furthermore, the substrates were immersed in 100 cm³ of the aqueous solution of 100 mmol dm⁻³ Cu(NO₃)₂, which was maintained at 351 ± 3 K without stirring in the dark or during light irradiation for 2 h. The substrates were washed with water after the Cu(NO₃)₂ treatment, dried at room temperature, then heated at 373, 473, 573, and 673 K for 2 h.

The TiO₂ powder (Nippon Aerosil, Tokyo, Japan, AEROXIDE TiO₂ P25), 1.00 g, was stirred in 100 cm³ of the aqueous solutions of 0.500, 1.00, 10.0, and 100 mmol dm⁻³ Cu(NO₃)₂ in the dark or during light irradiation for 10 min. The pH value in the solutions was adjusted to 4.6. The samples were washed with water after the Cu(NO₃)₂ treatment, dried at room temperature, then heated at 537 K for 2 h. In this case, the Ag particles were not deposited on the TiO₂ in order to prepare a very small amount of the CuO nanoparticles.

3.2. Measurements

Micromorphology, elemental mapping and composition analysis, X-ray diffraction patterns, BET specific surface areas, X-ray photoelectron spectra, and UV-Vis absorption and diffuse reflectance

spectra of the samples were obtained by the previously reported methods [17]. The total organic carbon (TOC) was measured using a wet chemical TOC analyzer (Shimadzu, Kyoto, Japan, TOC-VWP).

For evaluation of the photocatalytic properties, the photocatalyst powder samples, 50.0 mg, were added to 40.0 cm³ of 2.00×10^{-5} mol dm⁻³ aqueous solutions of MB (Wako, Osaka, Japan, S grade). The suspensions were stirred in the dark for 24 h and furthermore during the near-UV light irradiation from black light bulbs, as previously reported [17]. The UV-Vis absorption spectra of the MB in the centrifuged solutions were measured before and after the adsorption equilibrium and as a function of the light irradiation time using the spectrophotometer.

Each film or 5.0-mg powder sample was added to 50 cm³ of aqueous solution of terephthalic acid (3.0×10^{-3} mol dm⁻³, Wako, Osaka, Japan, S grade) and sodium hydroxide (1.0×10^{-2} mol dm⁻³). The solutions or suspensions were stirred in the dark for 24 h and furthermore during the UV irradiation from the black light bulbs. The terephthalic acid reacts with hydroxyl radical resulting from the photocatalytic reactions and produces 2-hydroxy terephthalic acid [26,27]. The fluorescence spectra of the 2-hydroxy terephthalic acid in the centrifuged solutions were obtained upon 312-nm excitation using a fluorescence spectrophotometer (Shimadzu, Kyoto, Japan, RF5300) as a function of the light irradiation time.

4. Conclusions

CuO particles were prepared from an aqueous solution of copper (II) nitrate at 351 K on the TiO₂ surface by a photocatalytic reaction and heating at 573 or 673 K. The CuO crystals with about 50–250 nm-sized particles were formed. NO₃⁻ was reduced to NO₂⁻ in the solution by the photocatalytic activity of the TiO₂, and water was simultaneously transformed into OH⁻. An increase in the basicity on the TiO₂ surface induced formation of a copper hydroxide. The copper hydroxide was then dehydrated and transformed into CuO by heating. The photocatalytic activity of the CuO-modified TiO₂ films were lower than that of the original TiO₂ film because the amount of the CuO was too great to enhance the charge separation. The TiO₂ loading a low amount of CuO, i.e., the submonolayer CuO and bare areas greater than 75% of the TiO₂ particle surface, demonstrated a higher photocatalytic activity for MB degradation compared to the original TiO₂ due to the electron transfer from the TiO₂ conduction bands to the CuO conduction band.

Supplementary Materials: The following are available online at <http://www.mdpi.com/2073-4344/9/4/383/s1>, Figure S1: EPMA element mapping images of the Ag-deposited TiO₂ film., Figure S2: XPS spectra related to the binding energy of the Cu 2p electrons for (1) the TiO₂ sample and the CuO-modified TiO₂ samples prepared using the (2) 0.500, (3) 1.00, (4) 10.0, and (5) 100 mmol dm⁻³ Cu(NO₃)₂ solutions., Figure S3: UV-Vis diffuse reflectance spectra of (1) the TiO₂ sample and the CuO-modified TiO₂ samples prepared using the (2) 0.500, (3) 1.00, (4) 10.0, and (5) 100 mmol dm⁻³ Cu(NO₃)₂ solutions., Figure S4: Changes in the methylene blue concentration during the UV irradiation using the TiO₂ sample and the CuO-modified TiO₂ samples prepared using the 0.500–100 mmol dm⁻³ Cu(NO₃)₂ solutions., Figure S5: Relative concentrations of methylene blue and TOC estimated by the UV-Vis absorption and TOC measurements, respectively, after the photocatalytic degradation for 60 min using the TiO₂ sample and the CuO-modified TiO₂ samples prepared using the 1.00 and 10.0 mmol dm⁻³ Cu(NO₃)₂ solutions., Figure S6: Time course of the fluorescence intensity of 2-hydroxy terephthalic acid in order to detect hydroxyl radicals produced during the UV irradiation using (1) the TiO₂ film and (2) the CuO-modified TiO₂ film prepared using the 100 mmol dm⁻³ Cu(NO₃)₂ solution and (3) the TiO₂ powder and (4) the CuO-modified TiO₂ powder prepared using the 1.00 mmol dm⁻³ Cu(NO₃)₂ solution.

Author Contributions: Investigation, N.H., S.Y., T.I., H.K., A.K. and T.Y.; supervision, H.N.; project administration, K.T.

Funding: This research was funded by JSPS KAKENHI Grant Numbers JP15K05472 and JP16KK0110.

Conflicts of Interest: The authors declare no conflict of interest.

References

1. Yang, J.; Wang, D.; Han, H.; Li, C. Roles of cocatalysts in photocatalysis and photoelectrocatalysis. *Acc. Chem. Res.* **2013**, *46*, 1900–1909. [[CrossRef](#)]
2. Ran, J.; Zhang, J.; Yu, J.; Jaroniec, M.; Qiao, S.Z. Earth-abundant cocatalysts for semiconductor-based photocatalytic water splitting. *Chem. Soc. Rev.* **2014**, *43*, 7787–7812. [[CrossRef](#)]
3. Zhou, X.; Wu, J.; Li, Q.; Zeng, T.; Ji, Z.; He, P.; Pan, W.; Qi, X.; Wang, C.; Liang, P. Carbon decorated In₂O₃/TiO₂ heterostructures with enhanced visible-light-driven photocatalytic activity. *J. Catal.* **2017**, *355*, 26–39. [[CrossRef](#)]
4. Bandara, J.; Udawatta, C.P.K.; Rajapakse, C.S.K. Highly stable CuO incorporated TiO₂ catalyst for photocatalytic hydrogen production from H₂O. *Photochem. Photobiol. Sci.* **2005**, *4*, 857–861. [[CrossRef](#)]
5. Choi, H.-J.; Kang, M. Hydrogen production from methanol/water decomposition in a liquid photosystem using the anatase structure of Cu loaded TiO₂. *Int. J. Hydrogen Energy* **2007**, *32*, 3841–3848. [[CrossRef](#)]
6. Li, G.; Dimitrijevic, N.M.; Chen, L.; Rajh, T.; Gray, K.A. Role of surface/interfacial Cu²⁺ sites in the photocatalytic activity of coupled CuO-TiO₂ nanocomposites. *J. Phys. Chem. C* **2008**, *112*, 19040–19044. [[CrossRef](#)]
7. Xu, S.; Sun, D.D. Significant improvement of photocatalytic hydrogen generation rate over TiO₂ with deposited CuO. *Int. J. Hydrogen Energy* **2009**, *34*, 6096–6104. [[CrossRef](#)]
8. Gombac, V.; Sordelli, L.; Montini, T.; Delgado, J.J.; Adamski, A.; Adami, G.; Cargnello, M.; Bernal, S.; Fornasiero, P. CuO_x-TiO₂ photocatalysts for H₂ production from ethanol and glycerol solutions. *J. Phys. Chem. A* **2010**, *114*, 3916–3925. [[CrossRef](#)]
9. Yu, J.; Ran, J. Facile preparation and enhanced photocatalytic H₂-production activity of Cu(OH)₂ cluster modified TiO₂. *Energy Environ. Sci.* **2011**, *4*, 1364–1371. [[CrossRef](#)]
10. Yu, J.; Hai, Y.; Jaroniec, M. Photocatalytic hydrogen production over CuO-modified titania. *J. Colloid Interface Sci.* **2011**, *357*, 223–228. [[CrossRef](#)]
11. Wang, Z.; Liu, Y.; Martin, D.J.; Wang, W.; Tang, J.; Huang, W. CuO_x-TiO₂ junction: what is the active component for photocatalytic H₂ production? *Phys. Chem. Chem. Phys.* **2013**, *15*, 14956–14960. [[CrossRef](#)]
12. Yang, R.; Yang, L.; Tao, T.; Ma, F.; Xu, M.; Zhang, Z. Contrastive study of structure and photocatalytic performance with three-dimensionally ordered macroporous CuO-TiO₂ and CuO/TiO₂. *Appl. Surface Sci.* **2014**, *288*, 363–368. [[CrossRef](#)]
13. Moniz, S.J.A.; Tang, J. Charge transfer and photocatalytic activity in CuO/TiO₂ nanoparticle heterojunctions synthesised through a rapid, one-pot, microwave solvothermal route. *ChemCatChem* **2015**, *7*, 1659–1667. [[CrossRef](#)]
14. Nagaya, S.; Nishikiori, H. Deposition of ZnO particles by photocatalytic reaction. *Chem. Lett.* **2012**, *41*, 993–995. [[CrossRef](#)]
15. Nishikiori, H.; Nagaya, S.; Takikawa, T.; Kikuchi, A.; Yamakami, T.; Wagata, H.; Teshima, K.; Fujii, T. Formation of ZnO thin films by photocatalytic reaction. *Appl. Catal. B* **2014**, *160–161*, 651–657. [[CrossRef](#)]
16. Nishikiori, H.; Fujiwara, S.; Miyagawa, S.; Zettsu, N.; Teshima, K. Crystal growth of titania by photocatalytic reaction. *Appl. Catal. B* **2017**, *217*, 241–246. [[CrossRef](#)]
17. Nishikiori, H.; Matsunaga, S.; Iwasaki, M.; Zettsu, N.; Yamakawa, M.; Kikuchi, A.; Yamakami, T.; Teshima, K. Formation of silica nanolayer on titania surface by photocatalytic reaction. *Appl. Catal. B* **2019**, *241*, 299–304. [[CrossRef](#)]
18. Sakai, N.; Fujishima, A.; Watanabe, T.; Hashimoto, K. Enhancement of the photoinduced hydrophilic conversion rate of TiO₂ film electrode surfaces by anodic polarization. *J. Phys. Chem. B* **2001**, *105*, 3023–3026. [[CrossRef](#)]
19. Sakai, N.; Fujishima, A.; Watanabe, T.; Hashimoto, K. Quantitative evaluation of the photoinduced hydrophilic conversion properties of TiO₂ thin film surfaces by the reciprocal of contact angle. *J. Phys. Chem. B* **2003**, *107*, 1028–1035. [[CrossRef](#)]
20. Nishikiori, H.; Tagami, K.; Matsunaga, S.; Teshima, K. In situ probing of photoinduced hydrophilicity on titania surface using dye molecules. *ACS Omega* **2019**, *4*, 5944–5949. [[CrossRef](#)]
21. Bovio, B.; Locchi, S. Crystal structure of the orthorhombic basic copper nitrate, Cu₂(OH)₃NO₃. *J. Crystallogr. Spectrosc. Res.* **1982**, *12*, 507–517. [[CrossRef](#)]

22. Di, L.; Duan, D.; Zhan, Z.; Zhang, X. Gas-liquid cold plasma for synthesizing copper hydroxide nitrate nanosheets with high adsorption capacity. *Adv. Mater. Interfaces* **2016**, *3*, 1600760. [[CrossRef](#)]
23. Schildermans, I.; Mullens, J.; Van der Veken, B.J.; Yperman, J.; Franco, D.; Van Poucke, L.C. Preparation and thermal decomposition of $\text{Cu}_2(\text{OH})_3\text{NO}_3$. *Thermochimica Acta* **1993**, *224*, 227–232. [[CrossRef](#)]
24. Zhang, T.; Oyama, T.; Aoshima, A.; Hidaka, H.; Zhao, J.; Serpone, N. Photooxidative N-demethylation of methylene blue in aqueous TiO_2 dispersions under UV irradiation. *J. Photochem. Photobiol. A* **2001**, *140*, 163–172. [[CrossRef](#)]
25. Zhang, T.; Oyama, T.; Horikoshi, S.; Hidaka, H.; Zhao, J.; Serpone, N. Photocatalyzed N-demethylation and degradation of methylene blue in titania dispersions exposed to concentrated sunlight. *Sol. Energy Mater. Sol. Cells* **2002**, *73*, 287–303. [[CrossRef](#)]
26. Hirakawa, T.; Nosaka, Y. Properties of $\text{O}_2^{\bullet-}$ and OH^\bullet formed in TiO_2 aqueous suspensions by photocatalytic reaction and the influence of H_2O_2 and some ions. *Langmuir* **2002**, *18*, 3247–3254. [[CrossRef](#)]
27. Hirakawa, T.; Yawata, K.; Nosaka, Y. Photocatalytic reactivity for $\text{O}_2^{\bullet-}$ and OH^\bullet radical formation in anatase and rutile TiO_2 suspension as the effect of H_2O_2 addition. *Appl. Catal. A* **2007**, *325*, 105–111. [[CrossRef](#)]



© 2019 by the authors. Licensee MDPI, Basel, Switzerland. This article is an open access article distributed under the terms and conditions of the Creative Commons Attribution (CC BY) license (<http://creativecommons.org/licenses/by/4.0/>).